A prudent adaptive behaviour accelerates disease transmission on networks
— Supplementary Information —

Samuel V. Scarpino,[1,2] Antoine Allard,[3] and Laurent Hébert-Dufresne[1]

[1] *Santa Fe Institute, Santa Fe, NM 87501, USA*
[2] *Department of Mathematics and Statistics and Complex Systems Center, University of Vermont, Burlington, VT 05405, USA*
[3] *Departament de Física Fonamental, Universitat de Barcelona, Barcelona 08028, Spain*

This document presents supplementary information related to the paper "A prudent adaptive behaviour accelerates disease transmission on networks". Section I offers a complete analysis and validation of the pairwise network model introduced in the paper. For the sake of completeness, the analysis given in the paper is reproduced. Section II validates the observed phenomenology of our model—i.e., the accelerating spread and bigger epidemics caused by relational exchange—using extensive numerical simulations. Finally, in Section III, we fit models with and without relational exchange to the state-level influenza data and found support for relational exchange in more than 400 influenza outbreaks.

I. ANALYSIS OF THE MODEL

A. Mass-action compartmental approach

The first model we discuss in the main text is a standard mass-action model where nodes are distinguished by their state in a Susceptible-Infectious-Recovered dynamics (variables in brackets correspond to the fraction of the population in each state). Since there is no way to distinguish the nodes before or after a substitution, the epidemic is simply described by the following system of equations

$$[\dot{S}] = \gamma[I] - \beta[S][I] \tag{1a}$$

$$[\dot{I}] = \beta[S][I] - (r+\gamma)\,[I] \tag{1b}$$

$$[\dot{R}] = r[I]\ . \tag{1c}$$

where r is the recovery rate, β is the transmission rate, and γ is the replacement rate. All variables in bracket are dynamical, and we use the dot notation to identify time derivative. In a mass action framework, without the ability to track relations, the model behaves exactly as a combination of SIS dynamics with recovery rate γ, and SIR dynamics with recovery rate r.

B. Network model with pair approximation

To adapt the relational exchange mechanism to network structures, we introduce pair approximations in the ODE system given by Eqs. (1). We now write

$$[\dot{S}] = -\beta\,[SI] \tag{2a}$$

$$[\dot{I}] = \beta\,[SI] - r[I] \tag{2b}$$

$$[\dot{R}] = r[I]\ , \tag{2c}$$

which is the standard SIR model, but written using *pairs* $[XY]$, defined as the *per capita* number of links between nodes in state X and Y. The time evolution of these pairs are governed by

$$[\dot{SS}] = \gamma\,[SI]\,\frac{[S]}{[S]+[R]} - 2\beta\,[SI]\,\frac{[SS]}{[S]} \tag{2d}$$

$$[\dot{SI}] = 2\gamma\,[II]\,\frac{[S]}{[S]+[R]} - (r+\gamma)\,[II] + \beta\,[SI]\left(2\frac{[SS]}{[S]} - \frac{[SI]}{[S]} - 1\right) \tag{2e}$$

$$[\dot{II}] = \beta\,[SI]\left(1+\frac{[SI]}{[S]}\right) - 2\,(r+\gamma)\,[II]\ , \tag{2f}$$

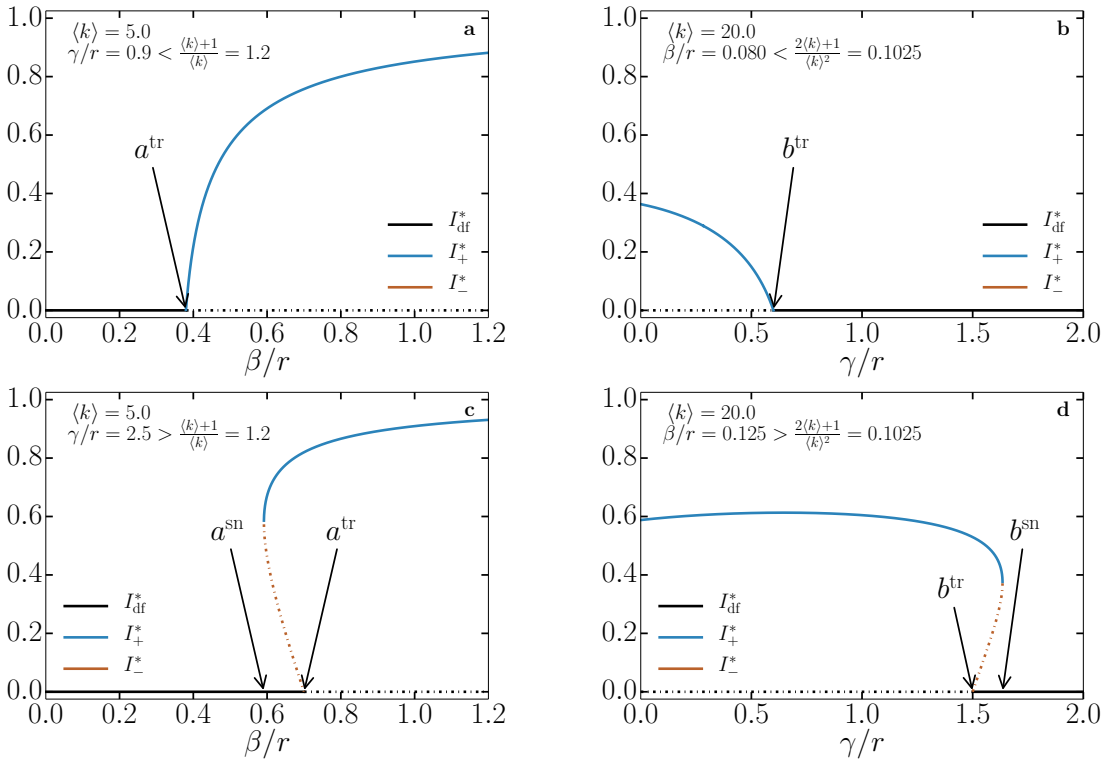

Supp. Fig. 1. Illustration of the theoretical predictions obtained for Eqs. (3). The solid lines show the stable branches of the possible steady states and the dashed lines show the unstable branches. The arrows point to the different threshold values obtained from Eqs. (15) and (17). The value of the fixed dimensionless parameter is also compared to the corresponding criterion given by Eq. (18).

where we have omitted the pairs $[XR]$ since they do not affect the dynamics of the model (i.e., they involve *inactive* recovered nodes). In this model, node states do not change following replacement [notice the absence of γ in Eqs. (2a)–(2c)]. However, links are rewired: e.g., $[SI]$ can become $[SS]$ if the infectious individual is replaced. The result is an adaptive network model where essential relations (e.g., patient-doctor, student-teacher) can be rewired.

To further simplify the analytical treatment, let us consider the SIS dynamics instead, which is described by

$$[\dot{S}] = r[I] - \beta\,[SI] \tag{3a}$$

$$[\dot{I}] = \beta\,[SI] - r[I]\,, \tag{3b}$$

which again is the standard SIS model, but written using pairs whose time evolution is governed by

$$[\dot{SS}] = (r+\gamma)\,[SI] - 2\beta\,[SI]\,\frac{[SS]}{[S]} \tag{3c}$$

$$[\dot{SI}] = (r+\gamma)\,(2\,[II] - [SI]) + \beta\,[SI]\left(2\frac{[SS]}{[S]} - \frac{[SI]}{[S]} - 1\right)\,, \tag{3d}$$

$$[\dot{II}] = \beta\,[SI]\left(1 + \frac{[SI]}{[S]}\right) - 2\,(r+\gamma)\,[II]\,. \tag{3e}$$

This model is similar to a variant of the adaptive network model introduced in Ref. [1] and further analysed in Ref. [2]. However, the adaptive process in their approach *always* hinders disease spread as the only possible adaptive move is from $[SI]$ to $[SS]$. In our model, there is an interesting trade-off between the positive effect of node replacement at the initial stages of the outbreak (i.e., from $[SI]$ to $[SS]$) and the negative impact it has once the disease is prevalent (i.e., from $[II]$ to $[SI]$).

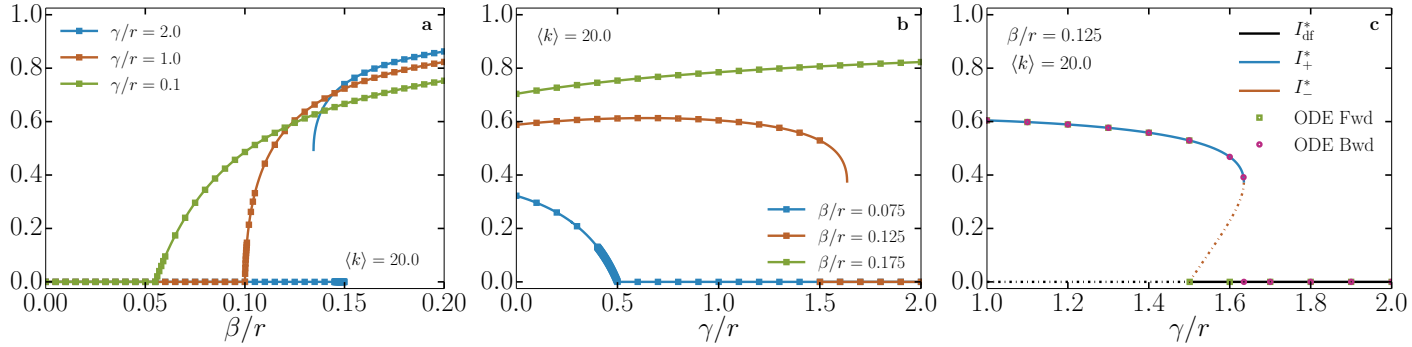

Supp. Fig. 2. (a-b) Steady-state prevalence, I^*, observed when fixing one of the two dimensionless parameters while varying the other one. The lines correspond to the analytical prediction of the stable steady states and symbols were obtained by integrating Eqs. (3) with the initial condition $I(0) = 0.0001$. The passage from a continuous to a discontinuous transition is clearly visible and happens in accordance to the criteria given by Eq. (18). (c) Validation of the bistable regime (in this case, when varying γ/r). The solid (dashed) lines show the stable (unstable) branches of the possible steady states, and the symbols show the value of the steady state observed when integrating Eqs. (3) with the initial condition $I(0) = 0.0001$ (ODE Fwd) and $I(0) = 0.9999$ (ODE Bwd).

Analytical solution of the network model with pair approximation

The evolution of the dynamical variables in the model is constrained by the conservation of nodes and links, namely

$$[S] + [I] = 1 \tag{4a}$$

$$[SS] + [SI] + [II] = \frac{\langle k \rangle}{2} \ , \tag{4b}$$

where $\langle k \rangle$ is the average degree of nodes in the network. These conditions imply that

$$[\dot{S}] + [\dot{I}] = 0 \tag{5a}$$

$$[\dot{SS}] + [\dot{SI}] + [\dot{II}] = 0 \ , \tag{5b}$$

which allows us to effectively reduce Eqs. (3) to the following system of three equations

$$[\dot{I}] = \beta\,[SI] - r[I] \tag{6a}$$

$$[\dot{SS}] = (r+\gamma)\,[SI] - 2\beta\,[SI]\,\frac{[SS]}{[S]} \tag{6b}$$

$$[\dot{II}] = \beta\,[SI]\left(1 + \frac{[SI]}{[S]}\right) - 2\,(r+\gamma)\,[II] \ . \tag{6c}$$

In other words, Eqs. (3a) and (3d) can be dropped since the conservation conditions, Eqs. (4), constrain the dynamics of variables $[S]$ and $[SI]$.

Steady state

We can readily see that a *disease-free* state, in which every node is susceptible,

$$[S]^*_{\rm df} = 1 \ ; \qquad [SS]^*_{\rm df} = \frac{\langle k \rangle}{2} \ ; \qquad [I]^*_{\rm df} = [SI]^*_{\rm df} = [II]^*_{\rm df} = 0 \ , \tag{7}$$

is a steady state of the pair-wise network model [Eqs. (4) and Eqs. (6)]. To see whether there exists another steady state, i.e., an *endemic* state in which a non-zero fraction of individuals are infectious, we set $[\dot{I}] = [\dot{SS}] = [\dot{II}] = 0$

in Eqs. (6). This yields

$$[SI]^*_\pm = \frac{[I]^*_\pm}{a} \tag{8a}$$

$$[SS]^*_\pm = \frac{1+b}{2a}(1-[I]^*_\pm) \tag{8b}$$

$$[II]^*_\pm = \frac{[I]^*_\pm}{2(1+b)}\left(1+\frac{[I]^*_\pm}{a(1-[I]^*_\pm)}\right) , \tag{8c}$$

where we have defined the dimensionless parameters $a \equiv \beta/r$ and $b \equiv \gamma/r$. Substituting these last equations in Eq. (4b), we obtain

$$\frac{1+b}{2a}(1-[I]^*_\pm) + \frac{[I]^*_\pm}{a} + \frac{[I]^*_\pm}{2(1+b)}\left(1+\frac{[I]^*_\pm}{a(1-[I]^*_\pm)}\right) = \frac{\langle k\rangle}{2} , \tag{9}$$

which can be rewritten as

$$\Big[b^2-a\Big][I]^{*\,2}_\pm + \Big[(b+1)(a\langle k\rangle-2b)+a\Big][I]^*_\pm + \Big[(b+1)(b+1-a\langle k\rangle)\Big] = 0 , \tag{10}$$

and whose solutions,

$$[I]^*_\pm = \frac{-\big[(b+1)(a\langle k\rangle-2b)+a\big] \pm \sqrt{a^2(b\langle k\rangle+\langle k\rangle-1)^2 - 4a(b+1)(b\langle k\rangle-1)}}{2(b^2-a)} , \tag{11}$$

correspond to the possible values of the endemic state. Note that only $[I]^*_-$ diverges when $a = b^2$ since $[I]^*_+$ converges towards

$$[I]^*_+ = 1 - \frac{1}{b(b+1)(b\langle k\rangle-1)-b} . \tag{12}$$

These solutions are illustrated on Suppl. Fig. 1.

Stability analysis and bifurcation

To determine whether the steady state solutions are stable or not, we linearize Eqs. (6) which yields the Jacobian matrix

$$\mathbf{J} = r\begin{pmatrix} -1 & -a & -a \\ -\dfrac{2a[SS][SI]}{(1-[I])^2} & -(1+b)-\dfrac{2a([SI]-[SS])}{1-[I]} & -(1+b)+\dfrac{2a[SS]}{1-[I]} \\ \dfrac{a[SI]^2}{(1-[I])^2} & -a-\dfrac{2a[SI]}{1-[I]} & -2(1+b)-a-\dfrac{2a[SI]}{1-[I]} \end{pmatrix} \equiv r\mathbf{J}' . \tag{13}$$

Notice that we have factorized[1] r from the matrix $\mathbf{J}$ to be able to work with the matrix $\mathbf{J}'$ expressed solely in terms of the dimensionless parameters a and b. Evaluating the matrix $\mathbf{J}'$ at a given steady state value $[I]^*$ [using Eqs. (8)] and calculating the real part of its largest eigenvalue $\lambda_{\max}$, we conclude that the steady state is stable if $\lambda_{\max} < 0$ and unstable if $\lambda_{\max} > 0$. Supplemental Figure 1 shows the stability/instability transitions of the steady states obtained by calculating the eigenvalues of $\mathbf{J}'$.

The disease-free steady state undergoes a transcritical bifurcation whenever either $[I]^*_+ = [I]^*_{\rm df} = 0$ or $[I]^*_+ = [I]^*_{\rm df} = 0$, which happens when the constant term in Eq. (10) equals to zero

$$(b+1)(b+1-a\langle k\rangle) = 0 . \tag{14}$$

[1] Multiplying a matrix by a scalar scales its eigenvalues by the same value. Consequently, both $\mathbf{J}$ or $\mathbf{J}'$ can equally be used to assess the stability of the steady states of Eqs. (6) since $r > 0$.

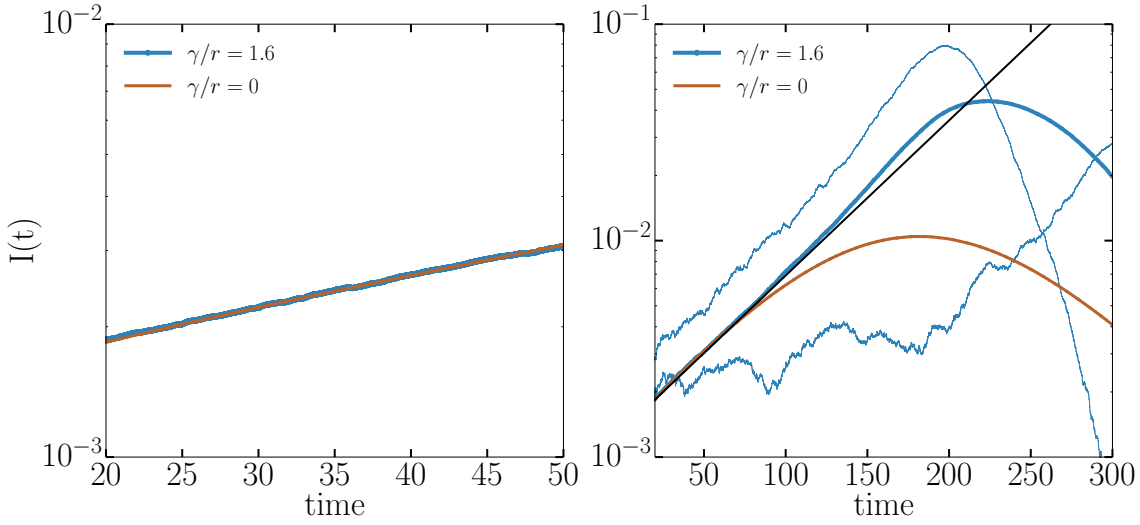

Supp. Fig. 3. **Simulations of relational exchange in a degree 4 regular network of 50,000 nodes.** We show the average state of all simulations (thick blue line) which used $r = 0.1$, $\beta = 0.1$ and $\gamma = 0.16$. We compare the results with a classic SIR model (orange line) that approximately gives the same exponential spread for early time values (left panel). What could have been our exponential fit on early data is presented in the right panel (black line). Notice both the accelerated spread and greater peak values than expected according to the classic model. We also show two time series of independent simulations (small blue dots) to illustrate how noisy the dynamics can be close to the discontinuity of the first-order transition. Hence, averaging over all simulations dampens the observed acceleration.

Fixing either a or b, we find the following threshold values

$$a^{\text{tr}} = \frac{b+1}{\langle k\rangle} \; ; \qquad b^{\text{tr}} = a\langle k\rangle - 1 \; . \tag{15}$$

Similarly, we see that the endemic steady state appears through a saddle-node bifurcation that occurs when $[I]^*_+ = [I]^*_-$ which, from Eq. (11), happens when

$$a^2(b\langle k\rangle + \langle k\rangle - 1)^2 - 4a(b+1)(b\langle k\rangle - 1) = 0 \; . \tag{16}$$

Fixing either a or b, we find the following threshold values[2]

$$a^{\text{sn}} = \frac{4(b+1)(b\langle k\rangle - 1)}{(b\langle k\rangle + \langle k\rangle - 1)^2} \; ; \qquad b^{\text{sn}}_{\pm} = \frac{-(\langle k\rangle - 1)(a\langle k\rangle - 2) \pm 2\sqrt{(\langle k\rangle + 1)^2 - a\langle k\rangle^2}}{\langle k\rangle(a\langle k\rangle - 4)} \; . \tag{17}$$

Notice that whenever $a\langle k\rangle = 4$, the threshold b^{sn}_- diverges but b^{sn}_+ equals $-1-1/\langle k\rangle(\langle k\rangle-1)$ which is always negative and therefore can be discarded. From Eqs. (15) and (17), we see that a bistable region appears or disappears when $a^{\text{tr}} = a^{\text{sn}}$ or $b^{\text{tr}} = b^{\text{sn}}_{\pm}$, which respectively yield the criteria

$$b > \frac{\langle k\rangle + 1}{\langle k\rangle} \; ; \qquad a > \frac{2\langle k\rangle + 1}{\langle k\rangle^2} \tag{18}$$

for the existence of a bistable region. These criteria are confirmed on Suppl. Fig. 1 and the complete analysis is validated on Suppl. Fig. 2.

II. SIMULATIONS AND VALIDATION

We validate the observed phenomenology of our model—i.e., the accelerating spread and bigger epidemics caused by relational exchange—in 3 simulated scenarios. We first use an initially degree-regular network and

[2] Whenever $a\langle k\rangle = 4$, the threshold b^{sn}_- diverges but b^{sn}_+ equals $-1 - 1/\langle k\rangle(\langle k\rangle - 1)$ which is always negative and therefore can be discarded.

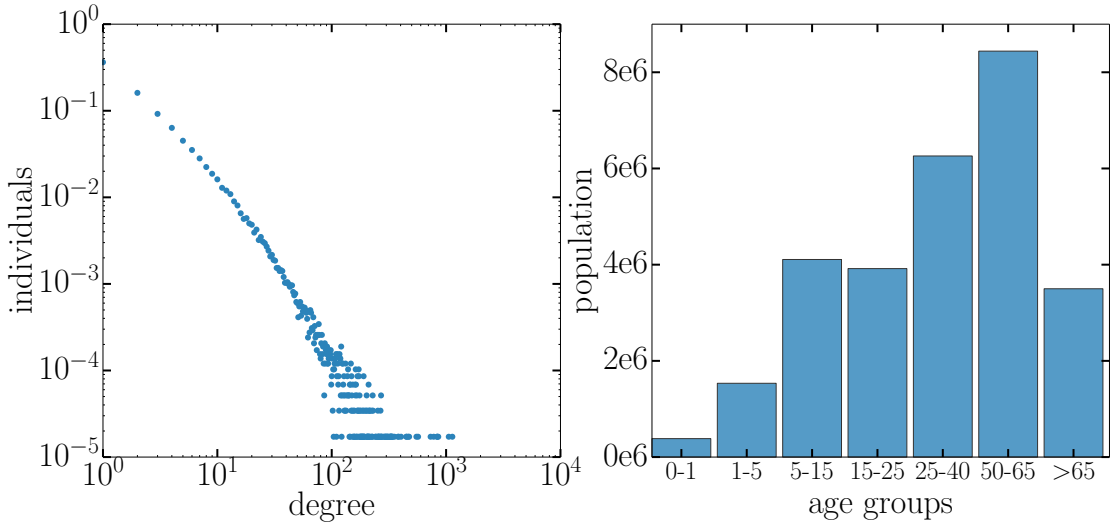

Supp. Fig. 4. **Degree and age distributions in our heterogeneous simulations.** (left panel) Degree distribution in location based online social network Brightkite [3]. The network consists of 58,228 users interconnected by 214,078 undirected edges. (right panel) Number of individuals per age class used for the simulations discussed in Sec. II C.

apply the exact process described by the ODE system [i.e., Eqs. (2)]. Second, we then change the initial topology to include heterogeneity by using real contact data from the location based online social network Brightkite [3]. We also take this opportunity to investigate the effect heterogeneity in relational exchange by having a sub-population where there is no relational exchange (e.g. children). Finally, we simulate a third and more complex model in which individuals are separated in age classes (where both population and contact frequency between classes are fixed by census data) and enforce a clustered work/school structure such that individuals go to work/school in the day and have a smaller, more intimate, contact network in the evening. In this case, all infected individuals are either aware or unaware of their status. If aware, an infected essential individual will simply not go to work and a substitute essential individual will take its place. This is designed to test the effect of more "realistic" social structure as well as *en masse* relational exchange (e.g. when sick, teachers have all links to their students exchanged to the substitute at once, not one by one, as in the ODE system).

A. Relational exchange in a degree-regular network

Our first set of simulations follows exactly the model described above. We start with a degree regular network where all nodes have exactly degree $k = 4$. We simulate the SIR dynamics, and allow individuals to randomly rewire their links to infectious individuals at rate γ. Results of our simulations are given on Supp. Fig. 3 and confirm the phenomenology observed in our analysis.

B. Heterogeneous relational exchange with heterogeneous degree distribution

Our second set of simulations uses the same dynamics but in a population with strong heterogeneity. First, we use data from the location based online social network Brightkite which features a fat-tail distribution (with scaling exponent around -2 and $\langle k \rangle = 7.35$, see Supp. Fig. 4). This heterogeneity implies a vanishing epidemic threshold, a higher peak in the presence of relational exchange would therefore suggest that our conclusions based on the analysis of the SIS model still hold. Second, we forbid 20% of the population from rewiring their own link. This is meant to represent "children" (or more broadly, young people with less responsibilities). The 20% figure is based on recent U.S.A census data for the population under 20. Their links with adults can still be rewired (e.g., from a teacher to their substitute) but not on their end (e.g., they do not get a substitute student if they do not show up to school). The results are presented in Supp. Fig. 5. The impacts of relational exchange are still present

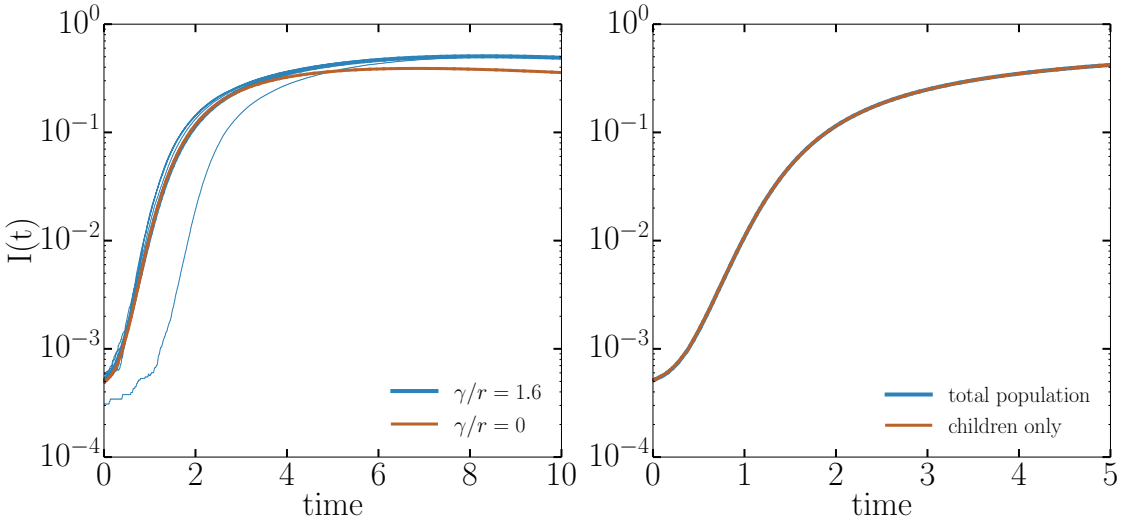

Supp. Fig. 5. **Simulations of relational exchange with children in an heterogeneous network.** (left panel) We show the average state of all simulations which used $r = 0.1$, $\beta = 0.1$ and $\gamma = 0.16$ (thick blue line) and $\gamma = 0$ (thick orange line). We again show a few random time series with relational exchange (small blue dots) to illustrate that there is still noise, and that averaging again dampens the acceleration (which is now mostly evident because of the higher peak prevalence). (right panel) We compare the total prevalence in the full population with the one observed in the subset corresponding to children. Even if the children, which correspond to 20% of the population, do not exchange their own relations, they are indistinguishable from the rest of the population because of their strong coupling with adults.

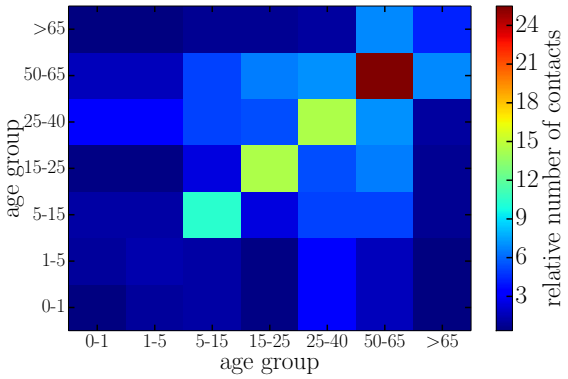

Supp. Fig. 6. **Mixing patterns between age classes.** Relative frequency of physical contacts between individuals of different age classes [4].

(slight acceleration and bigger peak prevalence), while there is virtually no impact of having a subpopulation without rewiring.

C. *En masse* relational exchange in a realistic network structure

We now use demographic data from the U.S.A. census to separate our population into 7 age classes, see Supp. Fig. 4. We then use empirical data on contact patterns between age groups [4] to impose a realistic mixing patterns, see Supp. Fig. 6. On top of those correlations, we enforce school/workplace clustering: Individuals between 5 and 25 years old are assigned to schools and are tagged as non-essential (as in the previous simulation). In schools, we enforce one essential adult per 10 children of age 5 to 15 years old, and one essential adult per 15 individuals of age between 15 and 25 years old. Other individuals above 25 are assigned to workplaces and 75% of them are tagged as essentials (security guards, cooks, retail workers, nurses, doctors, etc.). This leads to an heterogeneous

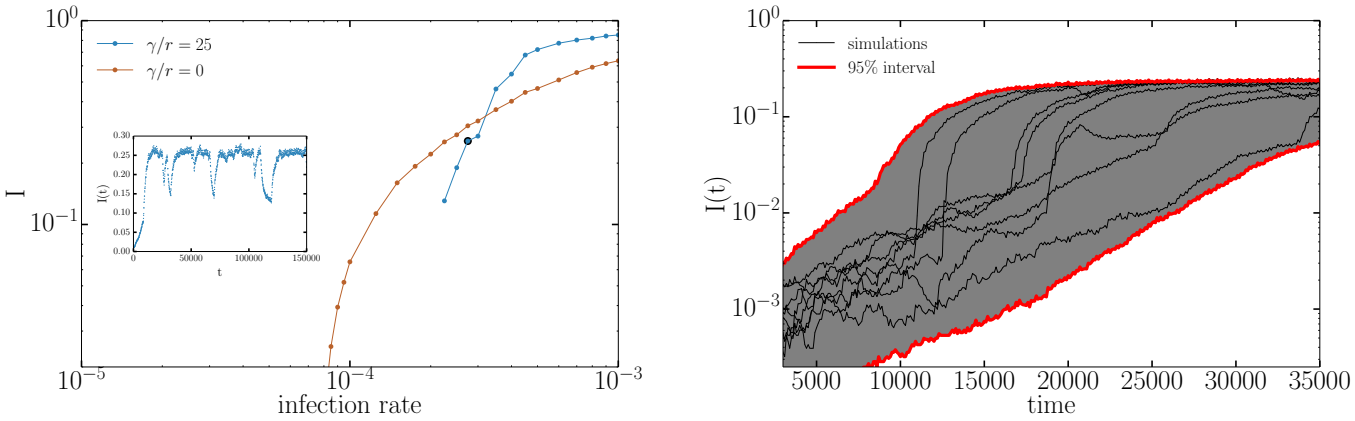

Supp. Fig. 7. **SIS epidemic phase transition in a complex social structure with relational exchange.** (left) We show the average steady state of simulations using $r = 0.001$ with $\gamma = 0.025$ (blue dots) and $\gamma = 0$ (orange dots) under variations of transmission rate β. We also show a time series with relational exchange and $\beta = 2.75 \times 10^{-4}$ (highlighted blue dot in main figure) in the inset to illustrate how the discontinuous transition and the hysteresis loop causes the heavy noise observed in the steady states. (right) The 95% intervals for time series with $\beta = 2.75 \times 10^{-4}$ are shown. Interestingly, the upper and lower bounds both show evidence of the acceleration due to relational exchange, but at different times and with different speed. This is again caused by the noise due to the nearby discontinuity. To show further evidence of this, we also plot several unique runs of the simulation which all show accelerations, but in very different forms.

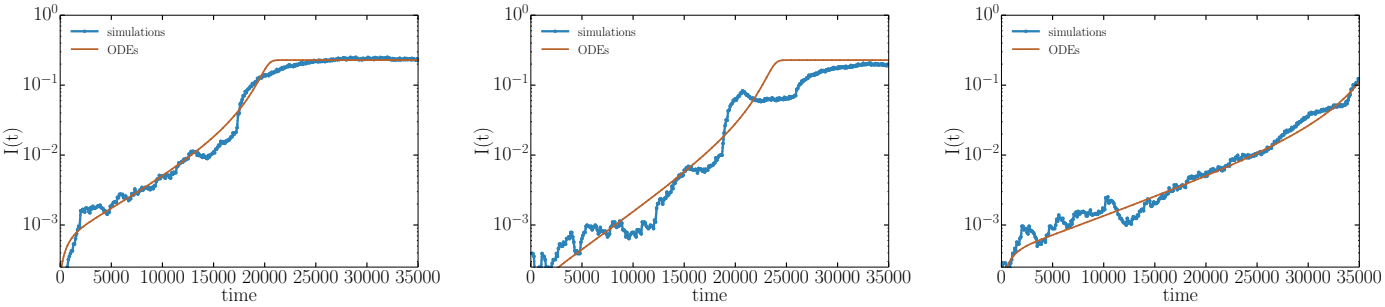

Supp. Fig. 8. **Noisy accelerations due to relational exchange in a complex social structure.** We use the parameters of the inset of Supp. Fig. 7 to produce time series of SIS dynamics in a complex social structure with relational exchange. These time series were chosen to represent three different cases, from left to right: early and drastic acceleration, very noisy acceleration and late acceleration. While quite noisy, the dynamics can be used to infer an *effective* relational exchange rate. Using the actual transmission and recovery rates, as well as the actual average degree from the simulations, we produce fits using our ODE system with γ equal to $3.3r$, $3.25r$, and $3.375r$ respectively from left to right.

network with an average degree $\langle k \rangle \simeq 18$. However, individuals have both a daytime set of connections and an evening one, which is a subset of the daytime network but about 5 times sparser. A vast majority of infections will thus occur during the day in the denser network. Essential infected individuals now become aware of their state at a rate γ, in which case their work relations are re-assigned to non-infected individuals from the same age group. Once they recover, essential individuals can then return to their original workplace.

In Supp. Fig. 7, we present the SIS epidemic transition on these realistic networks. As per the analysis of the main text, we see that without relational exchange, the system undergoes the classic continuous transition from a disease-free state to a steady state epidemic. And, as per our analysis with high relational exchange, the system now undergoes a discontinuous transition from the disease-free state to a large steady-state epidemic. This epidemic is initially smaller than expected without relational exchange, but eventually becomes *larger* than expected as the transmission rate is further increased, as predicted by our analysis. In the regime close to the discontinuous transition, our simulations predict very noisy behaviour, but very clear and strong accelerations.

Finally, we show how despite their differences and despite the fact that the model used here differ drastically from deterministic model considered in the main text, runs from our simulations can still be used to approximate

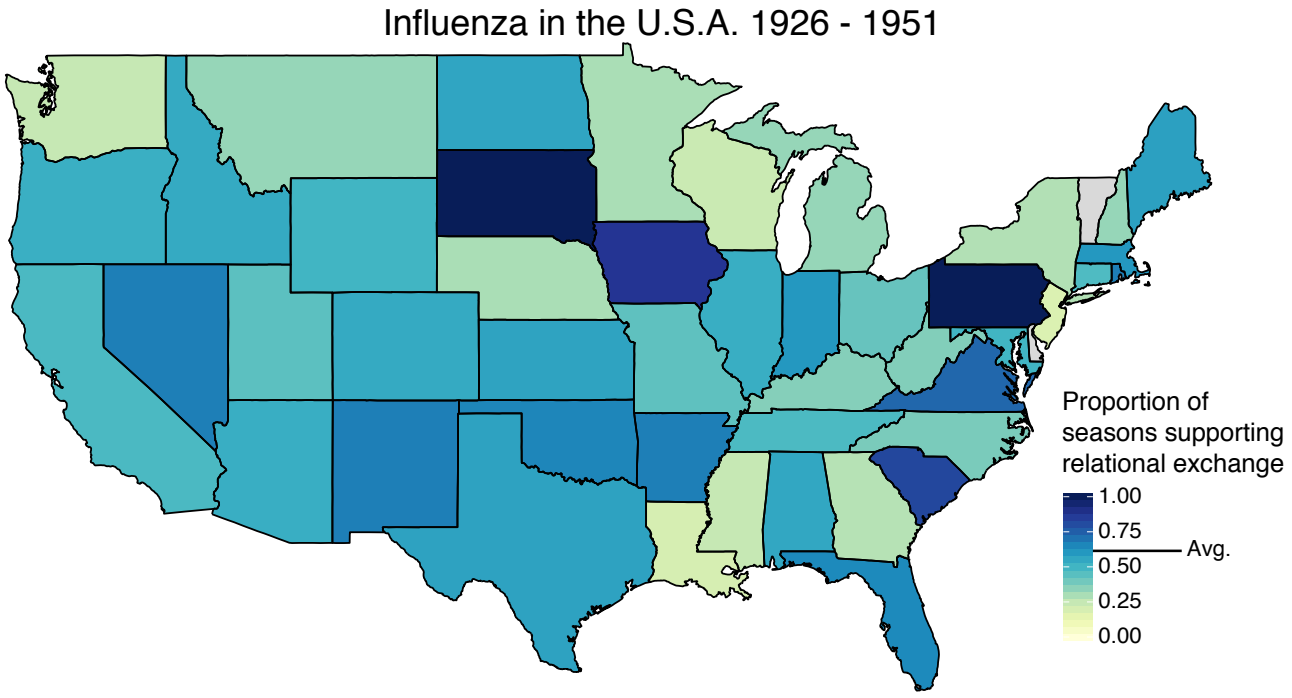

Supp. Fig. 9. **State-level empirical evidence for relational exchange.** A heatmap of the U.S.A. illustrating the proportion of influenza seasons between 1921 and 1951 showing evidence for relational exchange, with darker blues indicating more support than lighter blues and yellows. On average, over 55% of seasons across all states provide support for relational exchange. In comparison to the map in the main text, this means that we can use relational exchange to better forecast the influenza peak in 78% of cases when the outbreak deviates from the exponential spread. The data were obtained from the U.S.A. National Notifiable Diseases Surveillance System as digitized by Project Tycho.

an *effective* relational exchange rate. In Supp. Fig. 8, we take three time series from Supp. Fig. 7 that correspond to three different cases: early and drastic acceleration, very noisy acceleration and late acceleration. We roughly fit these time series to the ODE model using the actual transmission and recovery rates, the average degree from the simulations, as well as different initial conditions to account for stochasticity in the early time regime. What we find is three very similar values of relational exchange rate, varying only from $3.3r$ to $3.375r$. This shows that (i) our ODE model can be used to infer behavioural parameters even in scenarios with different microscopic mechanisms of relational exchange, and (ii) that despite the noise intrinsic to such adaptive dynamics, the inferred effective behavioural parameters can be quite consistent.

III. EMPIRICAL MODEL FITTING

To further strengthen our empirical findings, we fit two versions of the SIR network model with pair approximation, equations (2a), to all of the state-level influenza data. In version one of the model, we fix the replacement rate, γ at zero and estimate the transmission and recovery rates by performing a non-linear least-squares minimization using using the quasi-Newtonian gradient descent algorithm BFGS, as implemented in the R function "optim" in the stats library [5], R version 3.2.3; stats version 3.2.3. We further confirmed the quality of these minimization using simulated annealing on a subset of the model fits. In version two, we allow the replacement rate to take on non-zero values and fit the replacement, recovery, and transmission parameters using the procedure described above. Both versions of the model were solved using a backward differentiation formula that uses Jacobi-Newton iteration, as implemented in the "ode" function from the R package deSovle (v.1.13) [6]. For the initial conditions, we took the state population sizes as reported in the 1940 US census, the number of infectious individuals was set to the number of reported cases on week 0, and 95% of the population was assumed to be immune, i.e. in the recovered class. We used the same parameters for the degree distribution as those described above. We performed a limited set of sensitivity analyses and found that higher fractions of initially susceptible individuals led to increased support for the relational exchange model. Therefore, we felt our assumption of 5% susceptible

was conservative with respect to our goal of evaluating evidence for relational exchange. Again, we fit a subset of the models using simulated annealing and recovered similar parameter estimates and identical model selection results.

To evaluate each model, we fit to the first eight weeks of each influenza season and then projected the models forward through the second eight weeks. Each model was scored based on the out-of-sample root mean squared (RMSE). This out-of-sample RMSE allowed us to perform model selection, while simultaneous controlling for the additional free parameter in model 2. First, we find evidence for relational exchange in all seasons tested, meaning that the estimated value of γ was significantly greater than zero. Additionally, we find evidence that model 2, where replacement can take on non-zero values, is statistically the best model in over 55% of all season across all states, i.e. > 400 influenza outbreaks, see Supp. Fig. 9. This result of $> 55\%$ of influenza seasons supporting relational exchange closely matches our findings using the presence of exponential spread, where we found support in $> 70\%$ of seasons.

[1] Thilo Gross, Carlos J Dommar DLima, and Bernd Blasius, "Epidemic dynamics on an adaptive network," Physical review letters **96**, 208701 (2006).

[2] Vincent Marceau, Pierre-André Noël, Laurent Hébert-Dufresne, Antoine Allard, and Louis J Dubé, "Adaptive networks: Coevolution of disease and topology," Physical Review E **82**, 036116 (2010).

[3] Eunjoon Cho, Seth A Myers, and Jure Leskovec, "Friendship and mobility: user movement in location-based social networks," in *Proceedings of the 17th ACM SIGKDD international conference on Knowledge discovery and data mining* (ACM, 2011) pp. 1082–1090.

[4] Joël Mossong, Niel Hens, Mark Jit, Philippe Beutels, Kari Auranen, Rafael Mikolajczyk, Marco Massari, Stefania Salmaso, Gianpaolo Scalia Tomba, Jacco Wallinga, *et al.*, "Social contacts and mixing patterns relevant to the spread of infectious diseases," PLoS Med **5**, e74 (2008).

[5] R Core Team, *R: A Language and Environment for Statistical Computing*, R Foundation for Statistical Computing, Vienna, Austria (2015).

[6] Karline Soetaert, Thomas Petzoldt, and R. Woodrow Setzer, "Solving differential equations in r: Package desolve," Journal of Statistical Software **33**, 1–25 (2010).